

A Heterogeneous Pt-ReO_x/C Catalyst for Making Renewable Adipates in One Step from Sugar Acids

Jun Hee Jang, Insoo Ro, Phillip Christopher, and Mahdi M. Abu-Omar*

Cite This: *ACS Catal.* 2021, 11, 95–109

Read Online

ACCESS |



Metrics & More



Article Recommendations



Supporting Information

ABSTRACT: Renewable adipic acid is a value-added chemical for the production of bioderived nylon. Here, the one-step conversion of mucic acid to adipates was achieved in high yield through deoxydehydration (DODH) and catalytic transfer hydrogenation (CTH) by a bifunctional Pt-ReO_x/C heterogeneous catalyst with isopropanol as solvent and reductant. The Pt-ReO_x/C catalyst is reusable and was regenerated at least five times. The catalyst exhibits a broad substrate scope of various diols. Spectroscopic studies of Pt-ReO_x/C revealed Re^{VII} and Pt⁰ as the relevant species for DODH and CTH, respectively. Isotope labeling experiments support a monohydride mechanism for CTH over Pt. This work demonstrates a reusable bifunctional catalyst for a one-step valorization of sugar acids to a practical monomer, which opens the door to multifunctional catalysis streamlining valorization of biomass-derived molecules.

KEYWORDS: bifunctional catalysis, deoxydehydration, heterogeneous catalysis, hydrogen transfer, sugar acids



1. INTRODUCTION

Lignocellulosic biomass provides a renewable resource for sustainable routes to biofuels and biochemicals.^{1,2} Adipic acid is a large-volume, valuable chemical (1.8 €/kg) that can be obtained from biomass.³ Its primary use is in the production of nylon-6,6 with a global market size of 3.7 million tons per annum.⁴ The current manufacturing of adipic acid depends on petroleum-derived chemicals and emits nitrous oxide (N₂O).⁵ One promising route to renewable adipic acid is from biomass-derived C₆ carbohydrates. Glucose can be converted into *cis,cis*-muconic acid via biocatalysis, followed by direct hydrogenation over Pt/C to give adipic acid, as reported by Draths et al.^{6,7} The conversion of glucose derivatives including glucaric acid⁸ and 2,5-furandicarboxylic acid^{9,10} through chemocatalytic routes has also been studied. For example, Rennovia Inc. patented a process for the conversion of glucose to glucaric acid using Pd/SiO₂ catalyst. The resulting glucaric acid underwent hydrodeoxygenation to adipic acid using a bimetallic Pd-Rh/SiO₂ catalyst and a halogen source.⁸ However, these pathways from glucose and its derivatives either are low yielding (<30%) or employ undesirable reaction conditions such as requiring the use of corrosive halogens, a high pressure of H₂ (>50 bar), or acetic acid.

A combination of catalytic deoxydehydration (DODH) and hydrogenation offers an efficient and green route to adipates from mucic acid. Mucic acid (also known as galactaric acid) is an aldaric acid that can be produced by the oxidation of galactose.¹¹ A rhenium-catalyzed DODH reaction enables the selective conversion of vicinal diols to alkenes in the presence

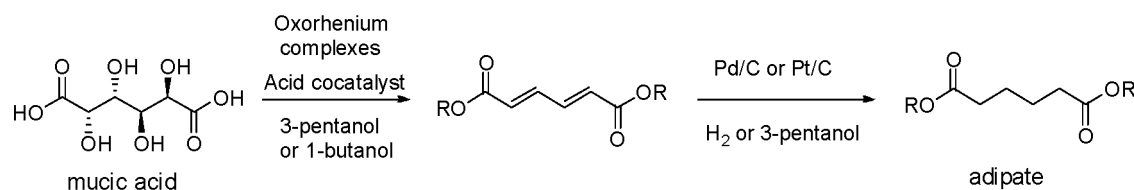
of reductants such as PPh₃, Na₂SO₄, H₂, and alcohols.^{12,13} High-oxidation-state rhenium catalysts and alcohol reductants have been widely studied for the DODH of various substrates, including sugar alcohols and acids. Homogeneous oxorhenium(VII) catalysts with *n*-butanol as solvent and reductant convert mucic acid to muconate through DODH (Scheme 1a). The following hydrogenation of muconate over Pd/C yields 62% adipates (Table S1).¹⁴ A higher yield (99%) of adipates can be obtained through two steps: (1) DODH by methyltrioxorhenium (MTO) and esterification over an acid cocatalyst and (2) catalytic transfer hydrogenation (CTH) over Pt/C.¹¹ In 2017, it was reported that a mixture of KReO₄, Pd/C, and phosphoric acid in combination with H₂ as a reductant yielded 86% adipates.⁵ Despite the high yield, the reaction system (homogeneous Re + heterogeneous Pt or Pd catalysts) presents challenging and likely costly separation and recycling problems. Due to the high cost of rhenium, employing a recyclable solid rhenium catalyst for DODH is desirable.¹⁵ Recently, a solid ReO_x/ZrO₂ catalyst with *n*-butanol as a reductant converted *D*-glucaric acid-1,4-lactone to muconate with a yield of 41% and another DODH product with a five-membered ring.¹⁶ When the product stream was

Received: September 22, 2020

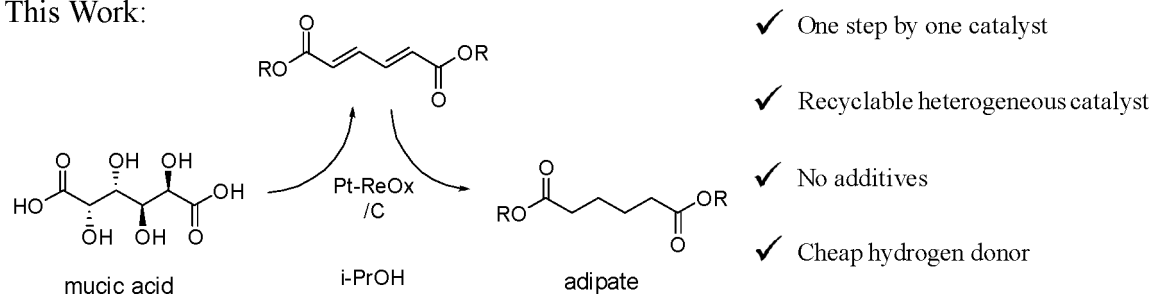
Revised: November 7, 2020

Scheme 1. DODH and Hydrogenation of Mucic Acid by (A) a Combination of Homogeneous Re and Heterogeneous Pd or Pt Catalysts in Multiple Steps and (B) a One-Step and Recyclable Catalyst

A) Previous Work:



B) This Work:



further processed via three different steps, including hydrogenation over Pd/C and ring opening, adipates were produced at 82% yield. While the yield of adipate is promising, the multistep process requires the isolation of intermediates and the use of different reaction conditions and catalysts.

In this work, we have designed a bifunctional heterogeneous catalyst that effectively catalyzes both DODH and CTH, converting mucic acid to adipates in one step. High-oxidation-state rhenium oxide on activated carbon (ReO_x/C) was chosen as a DODH catalyst. In order to catalyze the CTH reaction of C–C unsaturated bonds produced by the DODH reaction, metallic platinum was employed with the ReO_x/C , making a Pt- ReO_x/C catalyst. In the Pt- ReO_x/C catalyst, ReO_x and Pt are active sites for DODH and CTH, respectively. The role of Re in previously reported Pt-Re bimetallic catalysts was explained as a promoter for Pt catalysts.¹⁷ For example, in hydrocarbon reforming reactions over bimetallic Pt-Re catalysts, the addition of Re to Pt catalysts modified the electronic structure of Pt. This resulted in preventing carbon fouling and extending the lifetime of the catalyst.^{18–20} Furthermore, Pt-Re catalysts have shown increased activity for aqueous phase re-forming of biomass-derived polyols in comparison to monometallic Pt catalysts. This is attributed to Re promotion of Pt catalysts decreasing the binding energy of CO to the bimetallic surface and/or increasing the number of acid sites.^{21–23}

In addition to the separation and recycling problems, the aforementioned reaction systems (homogeneous + heterogeneous catalysts) require the use of acid additives and expensive alcohol reductants (C4 or higher) to achieve good yields of adipates. C4–C8 alcohols have been proven as effective reductants and solvents for the DODH reaction.^{13,24} Isopropanol is an attractive reductant for DODH because it is a cheap, green, and good solvent for reactants and products relative to the C4–C8 alcohols. For example, the ability of isopropanol to be a reductant and solvent for DODH was demonstrated for 1,2-hexanediol with an ammonium heptamolybdate (AMT) catalyst at high reaction temperatures (240–

250 °C).²⁵ However, MTO-catalyzed DODH did not proceed in isopropanol at 170 °C.²⁶ Moreover, the higher polarity of isopropanol relative to 3-octanol reduced the leaching problem of the $\text{ReO}_x/\text{support}$ catalyst during DODH.¹⁵ Re-diolate species, intermediate catalyst forms in the DODH cycle, are less soluble in more polar solvents. In addition to the advantages in DODH, isopropanol is a good hydrogen donor for the CTH reaction. CTH reactions using isopropanol as a hydrogen donor have garnered much attention as an alternative to direct hydrogenation because the hydrogen donor is easy to handle and environmentally friendly, minimizing possible hazards.^{27–29} While CTH reactions have been mostly accomplished using noble-metal complexes, several effective heterogeneous catalysts for the CTH of ketone, imines, and polarized alkenes have been reported.^{30–32}

Herein, we report the catalyst Pt- ReO_x/C for a one-step tandem catalysis of DODH and CTH (Scheme 1b). An 85% yield of adipates from mucic acid is achieved without an acid additive. Isopropanol is an effective solvent and hydrogen donor for both DODH and CTH reactions. On the basis of the reactivity, spectroscopic analysis, and isotope labeling experiments, a bifunctional mechanism of the tandem reaction is proposed. Catalyst recycling and regeneration are described.

2. EXPERIMENTAL DETAILS

2.1. Materials. All commercial materials were used as received. Ammonium perrhenate(VII) (Strem Chemicals) was purchased from Strem Chemicals. Hexachloroplatinic(IV) acid solution, nickel(II) nitrate, tetraamminepalladium(II) nitrate, iridium(III) chloride, activated carbon (Darco 100 mesh), D-sorbitol, D-glucaric acid-1,4-lactone, and (R,R)-(+)-hydrobenzoin were purchased from Sigma-Aldrich. Tris-(ethylenediamine)rhodium(III) chloride, methanol, ethanol, isopropanol, 1-butanol, 3-pentanol, glycerol, D-sorbitol, mucic acid, and L-(+)-tartaric acid were purchased from Alfa Aesar. Diisopropyl L-(+)-tartarate, diisopropyl fumarate, and diisopropyl succinate were purchased from TCI Chemicals.

Isopropanol-2- d_1 was purchased from Cambridge Isotope Laboratory.

2.2. Catalyst Preparation. The catalyst ReO_x/C was prepared by wet impregnation of an ammonium perrhenate aqueous solution. A 72 mg portion of ammonium perrhenate was dissolved in 4 mL of distilled water. A 1 g portion of activated carbon was mixed vigorously with the perrhenate solution overnight. After water was evaporated in a preheated 80 °C oil bath for 1.5 h and the residue dried in a 120 °C oven overnight, the catalyst was dehydrated at 480 °C for 4 h (heating rate of 8 °C/min) under flowing N_2 . Bifunctional catalysts ($\text{M-ReO}_x/\text{C}$, $\text{M} = \text{Ni}, \text{Pd}, \text{Ru}, \text{Rh}, \text{Ir}, \text{Pt}$) were synthesized by impregnating the metal precursor solution with the prepared ReO_x/C . The M/Re molar ratio was fixed to 0.4. For $\text{Pt-ReO}_x/\text{C}$, 500 mg of the synthesized ReO_x/C was mixed with 263 mg of 8 wt % hexachloroplatinic(IV) acid solution and 2 mL of distilled water. The catalyst $\text{Pt-ReO}_x/\text{C}$ was used after removing water in an oil bath at 80 °C, drying at 120 °C overnight, and dehydrating ($\text{N}_2/480$ °C/2 h). The monometallic Pt/C catalyst was prepared by the same impregnation method with hexachloroplatinic acid. All catalysts were used and characterized without the treatment of reduction unless otherwise noted.

2.3. Characterization. High-angle annular dark-field scanning transmission electron microscope (HAADF-STEM) images were collected at 200 kV using a Thermo Scientific Talos instrument equipped with a Super-X detector system. The samples were diluted in ethanol and deposited on a carbon film copper grid. In order to explore the distribution of ReO_x and Pt, energy-dispersive X-ray spectroscopy (EDX) mapping was performed on the distribution of Re, Pt, and O elements. The average particle size of $\text{Pt-ReO}_x/\text{C}$ was calculated from the STEM images. Transmission electron microscope (TEM) images of ReO_x/C were obtained on an FEI Tecnai G2 microscope.

X-ray photoelectron spectroscopy (XPS) analysis was acquired on a ThermoFisher Escalab Xi+ instrument with a monochromatic Al $K\alpha$ X-ray source. High-resolution spectra (20 eV) of Re 4f, Pt 4f, C 1s, and O 1s and the survey spectra (100 eV) were recorded. All of the spectra were calibrated by setting the binding energy of the peak of C 1s to 284.5 eV. CasaXPS software was utilized to deconvolute the spectra. The catalyst $\text{Pt-ReO}_x/\text{C}$ prepared by the method described above was analyzed without further treatment. The samples after the reaction, reduction, and regeneration were transferred to a glovebox filled with N_2 , avoiding exposure to air. The samples were mounted on a transfer vessel in the glovebox and transferred to the XPS chamber without air exposure.

X-ray diffraction (XRD) patterns were collected from 2θ range of 5–80° on a PANalytical Empyrean X-ray diffractometer using Cu $K\alpha$ radiation. Inductively coupled plasma (ICP) analysis was carried out to quantify the amount of metal using a Thermo iCAP 6300 instrument. For the sample preparation, 20 mg of catalyst was digested with 2.5 mL of aqua regia by refluxing at 150 °C for 6 h. The solution was cooled to room temperature, filtered, diluted, and used for ICP analysis. Because the catalysts after reaction contain organic deposits, they were regenerated under 5% H_2 in Ar at 230 °C for 4 h before the acid digestion.

The CO chemisorption studies were carried out using a Micromeritics AutoChem II 2920 instrument. The as-prepared catalysts were pretreated under an Ar flow at 450 °C for 2 h, and CO adsorption was performed at 35 °C. The adsorption

stoichiometry between CO and surface Pt sites was assumed to be 1:1. The catalysts after the reaction were pretreated under an Ar or H_2 flow and used for CO chemisorption. Temperature-programmed reduction (TPR) was carried out using a Micromeritics AutoChem II 2920 instrument. Before TPR, samples were pretreated under an Ar flow at 400 °C for 4 h. A TPR run was carried out in a flow of 10% $\text{H}_2/90\%$ Ar gas mixture at a flow rate of 50 mL min^{-1} with a temperature ramp of 10 °C min^{-1} . The consumption of hydrogen was monitored as a function of temperature using the TCD.

Infrared spectra of catalysts were recorded with a Thermo Scientific Nicolet iS10 Fourier transform infrared (FTIR) spectrometer with a mercury cadmium telluride detector cooled by liquid nitrogen. Catalysts were diluted with KBr. Before characterization, catalysts were pretreated in situ under an Ar flow at 400 °C for 4 h. After pretreatment, the catalysts were cooled to room temperature under Ar, and then a baseline spectrum was taken before pyridine introduction. Pyridine was introduced to the catalyst by flowing Ar through a pyridine bubbler, and then the system was purged with 100 sccm of Ar for 10 min to remove physisorbed pyridine. For all measurements, spectra were obtained by averaging 64 sequentially collected scans at a resolution of 4 cm^{-1} .

2.4. General Catalytic Procedure. The $\text{Pt-ReO}_x/\text{C}$ catalyst (150 mg), mucic acid (1 mmol, 210 mg), and isopropanol (40 mL) were placed in a Parr vessel. The vessel was pressurized with nitrogen to 15 bar and heated to 170 °C. After 6 h of reaction, the reactor was cooled and the gases were collected in a gas sample bag. The used catalyst was filtered, washed with pure isopropanol (30 mL), and dried in the oven at 120 °C overnight for recycling tests. The reaction solution was concentrated under reduced pressure, and the products were dissolved in d_6 -DMSO and analyzed by NMR with benzaldehyde as an internal standard. ^1H NMR and ^{13}C NMR spectra were collected on an Agilent Technologies 400 MHz, 400-MR DD2 spectrometer. The gas phase was analyzed by GC-TCD (Shimadzu GC-9AIT with a Shincarbon ST column), GC-MS (Shimadzu GC-2010 with a DB-1 capillary column coupled to a QP2010 MS), and GC-FID (Shimadzu GC-2010 equipped with a Supelco alumina sulfate column) with 1-butene as an internal standard. The recycling test of the $\text{Pt-ReO}_x/\text{C}$ for the 6 h DODH-CTH reaction was conducted with or without regeneration under H_2 . For regeneration, the used and recovered catalyst was treated at 230 °C for 4 h in a flow of H_2 (5%) in Ar and reoxidized in a 120 °C oven for 1 h. During the recovery step, a slight weight loss of less than 10 wt % was observed. Thus, the amounts of mucic acid and isopropanol in each reuse experiment were determined on the basis of the amount of the recycled catalyst.

2.5. Stability Test. Diisopropyl L-(+)-tartarate and diisopropyl fumarate were used as substrates for the stability tests due to their good solubility in isopropanol. DODH of diisopropyl L-(+)-tartarate gave diisopropyl fumarate and CTH of diisopropyl fumarate produced diisopropyl succinate. These diester compounds in the product solution were analyzed with GC-FID (Agilent Technologies 6890N instrument with a DB-5 capillary column) with mesitylene as an internal standard. A 4 mmol amount of the substrate, 100 mg of $\text{Pt-ReO}_x/\text{C}$ catalyst, 200 mg of activated carbon, and 40 mL of isopropanol were loaded into the reaction vessel, and the vessel was pressurized with 15 bar of N_2 . The reaction started once the temperature reached 170 °C. After 20 min, the reaction was stopped and quenched in an ice/water bath. The used catalysts

Table 1. DODH and CTH Tandem Reaction of **1** over ReO_x/C^a

R = H or isopropyl

entry	reductant	T (°C)	t (h)	conversion ^b (%)	product selectivity (%) ^b			
					2	3 and 4	5	others
1	isopropanol	170	6	77	86	2	0	12
2	isopropanol	170	12	94	75	13	1	11
3	isopropanol	230	24	100	0	19	35	46
4	methanol	170	12	88	60	13	0	27
5	ethanol	170	12	94	66	14	0	20
6	3-pentanol	170	12	83	87	0	0	13

^aReaction conditions: ReO_x/C (150 mg, 4.5 wt % Re), **1** (1 mmol), *i*-PrOH (40 mL), and N_2 (15 bar). ^bConversion and selectivity were calculated by ¹H NMR.

were separated and washed with 30 mL of isopropanol and dried overnight in a 120 °C oven. The amounts of mucic acid and isopropanol in each reuse experiment were determined on the basis of the amount of the recycled catalyst. The regeneration step (5% $\text{H}_2/230$ °C/4 h) including reoxidation was employed after deactivation was observed.

3. RESULTS AND DISCUSSION

3.1. DODH Reaction. The heterogeneous oxorhenium-catalyzed DODH reaction, as an alternative to homogeneous DODH, has attracted much attention due to process advantages.^{15,33–37} Oxorhenium supported on activated carbon (ReO_x/C) is an active catalyst for DODH with 3-octanol as a reductant.³⁵ Recently, this catalyst also promoted the CTH reaction with isopropanol for C–O cleavage of lignin model compounds.³⁸ In this study, the ability of isopropanol to act as a reductant and solvent for both DODH and CTH catalyzed by a heterogeneous ReO_x/C catalyst was investigated. The ReO_x/C catalyst with 4.5 wt % of Re was prepared by a wet impregnation method with ammonium perrhenate as a precursor. The ReO_x nanoparticle size ranges from 1 to 4 nm (Figure S1). In 6 h, ReO_x/C with isopropanol converted 77% of mucic acid (**1**) to muconic acid and its esters (**2**) with a high selectivity of 86% (entry 1 in Table 1), showing the high DODH ability of ReO_x/C and isopropanol. To the best of our knowledge, this is the first report to demonstrate isopropanol as an effective solvent and reductant for the rhenium-catalyzed DODH reaction. After 12 h, conversion reached 94%, producing not only **2** but also hydrogenated products (**3–5**). CTH proceeded to some extent (14% selectivity of **3/4** and **5**), even with ReO_x/C alone (entry 2). DODH in 3-pentanol also displayed high selectivity for **2**, but further hydrogenation was not observed (entry 6). Lower selectivity for **2** was obtained in methanol and ethanol (entries 4 and 5). Thus, among the tested C1–C5 secondary alcohols, isopropanol was found to be the most effective hydrogen donor for DODH and CTH over ReO_x/C .

The heterogeneous catalyst ReO_x/C with isopropanol did not require an acid additive and showed a higher DODH turnover frequency per Re atom (3.1 h^{-1}) in comparison to MTO and *p*-toluenesulfonic acid with 3-pentanol (1.7 h^{-1} , entry 2 in Table S1). It was previously reported that the addition of a Brønsted acid promotes the esterification of **1**,

resulting in the enhanced solubility of mucic acid.¹¹ In the absence of *p*-toluenesulfonic acid, the turnover frequency per Re atom in the homogeneously catalyzed system decreased to 0.9 h^{-1} . While the addition of a Brønsted acid to ReO_x/C increased the number of ester groups, it did not increase the conversion or selectivity of **2** (Figure S2 and Table S2). This indicates that the reactant solubility has little effect on the turnover frequency per Re atom of DODH over the solid ReO_x/C catalyst. Weak Lewis acid sites in ReO_x/C were detected by pyridine probe-molecule FT-IR (Figure S3). However, addition of exogenous Lewis acids such as ZnCl_2 had no effect on the conversion or selectivity, indicating negligible involvement of the Lewis acid sites of ReO_x/C in the DODH reaction (Table S2).

Despite the high conversion and selectivity of DODH over ReO_x/C with isopropanol, CTH was quite slow at 170 °C (Table 1, entry 2). Four different temperatures from 170 to 230 °C were investigated to convert *trans,trans*-muconic acid (**2**-diacid) to **5** through CTH (Figure S4). The highest yield of **5** (43%) was obtained at 230 °C. However, the elevated temperature also resulted in 35–50% byproducts including oxepane (**6**), alkylated adipates (**7**), and other unidentified products. As a result, the higher temperature conversion of **1** led to a moderate yield of **5** (35%) and several other products (entry 3 in Table 1).

3.2. Bifunctional Catalysis. A bifunctional catalyst provides two different catalytic sites for a consecutive reaction ($\text{A} \rightarrow \text{B} \rightarrow \text{C}$).^{39,40} To realize high efficiency for both DODH and CTH, several bimetallic catalysts ($\text{M-ReO}_x/\text{C}$) were prepared by a sequential impregnation method and evaluated for mucic acid conversion (Figure 1 and Table S3). Among them, Pt- ReO_x/C showed the highest conversion (79%) and selectivity for adipates (82%, entry 1 in Table 2). The bimetallic catalysts containing Ni and Pd did not promote the CTH reaction. Some hydrogenated products (**3/4** and **5**) were obtained by adding Ru, Ir, and Rh to ReO_x/C , but the reactant conversion was low. The addition of Pt to ReO_x/C significantly enhanced the selectivity of **5** while maintaining the excellent DODH ability of ReO_x/C (Figure 1 and entries 1 and 7 in Table S3). The carbon balance after 6 h of the DODH-CTH reaction over Pt- ReO_x/C catalyst is described in Table S4. The sum of C6 reactant and products (**1–5**) exhibited 92% carbon balance, and remaining 8% could be explained by organic deposits, which are discussed in a later

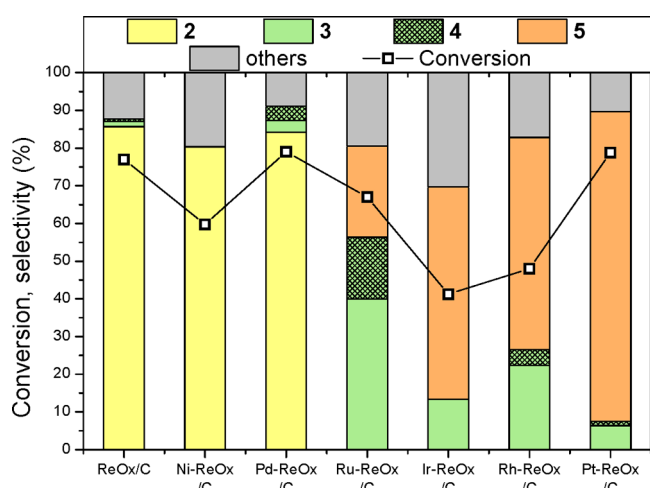


Figure 1. Conversion of 1 over several bimetallic catalysts. Reaction conditions: 1 (1 mmol), M-ReO_x/C (150 mg), isopropanol (40 mL), N₂ (15 bar), 170 °C, 6 h.

section. During the 6 h reaction, 5.5% of isopropanol was converted, offering hydrogen for both DODH and CTH and producing C3 products, including acetone. The higher amount of acetone (5.2 mmol) produced in comparison to the theoretically required amount of H₂ (2.8 mmol) indicated the independent dehydrogenation of isopropanol by Pt-ReO_x/C. A 1.2 mmol amount of molecular hydrogen was detected by GC-TCD analysis of the gas phase (Figure S5). The produced acetone can be rehydrogenated to isopropanol with hydrogenation catalysts. For example, Raney nickel catalyst showed 99.9% conversion of acetone and 99.9% selectivity of isopropanol in the liquid phase.⁴¹ In addition to the conversion of isopropanol to acetone, dehydration of isopropanol also occurred, producing some of propene (0.2 mmol) and diisopropyl ether (1.8 mmol) in the reaction solution (Table

S4). Gas product analysis by GC-MS and GC-FID with 1-butene as an internal standard can quantify propene (0.12 mmol), propane (0.32 mmol), and isopropanol (0.06 mmol) in the gas phase. On the basis of the liquid- and gas-phase analysis and the conversion of isopropanol, the C3 carbon balance reached 96% (Table S4).

Monometallic Pt/C by itself was inactive for DODH (entry 6 in Table 2), but with 2-diacid as a substrate, quantitative conversion to 5 was observed (99% yield). The product selectivity was sensitive to Pt loading (entry 7). A higher Pt loading (4.5 wt %) was detrimental because ReO_x active sites were blocked, lowering conversion of 1 (entry 8). A 1.8 wt % Pt loading along with 4.5 wt % Re was identified as an optimal composition for DODH and CTH. CTH over Pt-ReO_x/C in isopropanol was observed to be superior to that in 3-pentanol (entry 9).

The time profile of the DODH-CTH reaction over Pt-ReO_x/C is shown in Figure 2 (see also Figure S6). It follows a sequential kinetic scheme of DODH followed by two steps of CTH: 1 → 2 → 3/4 → 5. It is notable that both intermediates 2 and 3/4 were observed along the path of the reaction, indicating that CTH proceeded at rates similar to those of DODH. After 24 h, an 85% overall yield of 5 was attained. 5 contains adipic acid (30%) and isopropyl esters (70%), quantified by ¹H and ¹³C NMR (Figure S7). Acid hydrolysis of the products gave isolated adipic acid in 77% yield (Figure S8). The reaction concentration increased from 0.025 to 0.1 to 0.25 M (entries 1–3 in Table 3). In DODH-CTH with the higher concentration solution, the selectivity of 5 decreased mainly due to the side reactions and byproducts. The most probable side reaction was intramolecular dehydration of 1 to cyclic compounds and following DODH-CTH could make the cyclic byproducts shown in Scheme S1. The side reactions could be suppressed by using diisopropyl mucate (13) as a substrate, showing a high selectivity of 5 (83%) even in the higher concentration solution of 0.25 M (entry 4 in Table 3).

Table 2. DODH-CTH Tandem Reaction of 1 over Pt-ReO_x/C^a

R = H or isopropyl

entry	catalyst	Re/Pt amount (wt %)	conversn ^b (%)	product selectivity (%) ^b			
				2	3 and 4	5	others
1	Pt-ReO _x /C	4.5/1.8	79	0	7	82	11
2 ^c	2nd cycle		64	1	50	40	9
3 ^d	3rd cycle		77	0	10	82	8
4 ^d	4th cycle		72	0	19	77	4
5 ^e	5th cycle		81	0	6	83	11
6	Pt/C	0/1.8	no reaction				
7	Pt-ReO _x /C	4.5/0.9	78	42	44	5	9
8	Pt-ReO _x /C	4.5/4.5	44	0	9	71	20
9 ^f	Pt-ReO _x /C	4.5/1.8	73	90	7	0	3
10 ^g	ReO _x /C + Pt/C	4.5/1.8	78	0	3	83	14
11 ^c	2nd cycle		48	0	4	85	11

^aReaction conditions unless specified otherwise: 170 °C, 6 h, 1 (1 mmol), catalyst (150 mg), *i*-PrOH (40 mL), N₂ (15 bar). ^bConversion and selectivity were calculated by ¹H NMR. ^cWithout regeneration. ^dRegeneration conditions: H₂/230 °C/2 h and reoxidation (air/120 °C/1 h). ^eRegeneration conditions: H₂/230 °C/4 h and reoxidation (air/120 °C/1 h). ^f3-pentanol (40 mL). ^g1.8 wt % Pt/C (150 mg) + 4.5 wt % ReO_x/C (150 mg).

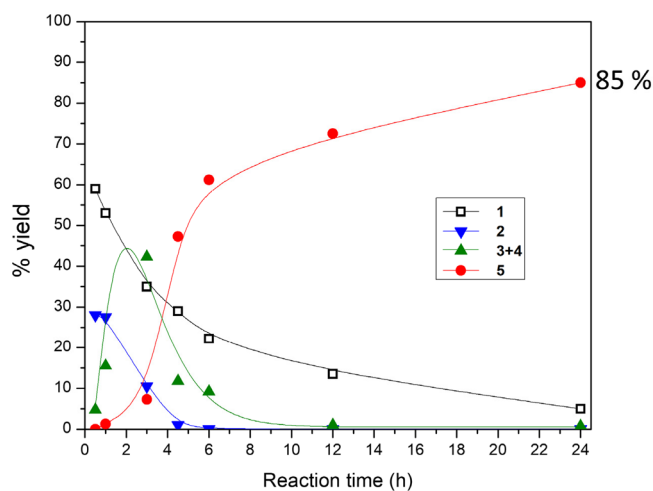


Figure 2. Reaction profile of DODH-CTH tandem reaction of **1** over Pt-ReO_x/C. Reaction conditions: **1** (1 mmol), Pt-ReO_x/C (150 mg), isopropanol (40 mL), N₂ (15 bar), 170 °C. The solid lines are to guide the eye. Because the reaction time was counted after the inside temperature reached 170 °C, some amount of **1** was converted to **2** before the reaction time started.

3.3. Catalyst Characterization. Pt-ReO_x/C was characterized by microscopy- and spectroscopy-based methods. STEM combined with EDX analysis showed that Pt and Re existed on the same particles (Figure 3 and Figure S9). Even though each particle contains both Re and Pt, the Pt/Re peak ratio is not uniform, suggesting different compositions within particles (Figure S9). The average particle size of Pt-ReO_x/C calculated from STEM images is 3.2 ± 1.5 nm (Figure S9c), which is larger than that of ReO_x/C (2.2 ± 0.4 nm, Figure S1). This indicates the formation of larger particles when Pt is added to ReO_x/C.

H₂-TPR profiles of monometallic and bimetallic catalysts were analyzed to investigate the interaction between Re and Pt (Figure 3e). The peak at a high temperature of around 600 °C is due to methanation of the carbon support with H₂.^{42,43} The TPR result of Pt/C exhibits a uniform reduction peak at 303 °C, which is assigned to the reduction/decomposition of Pt^{II} species shown in XPS results of Pt/C below. Previous TPR

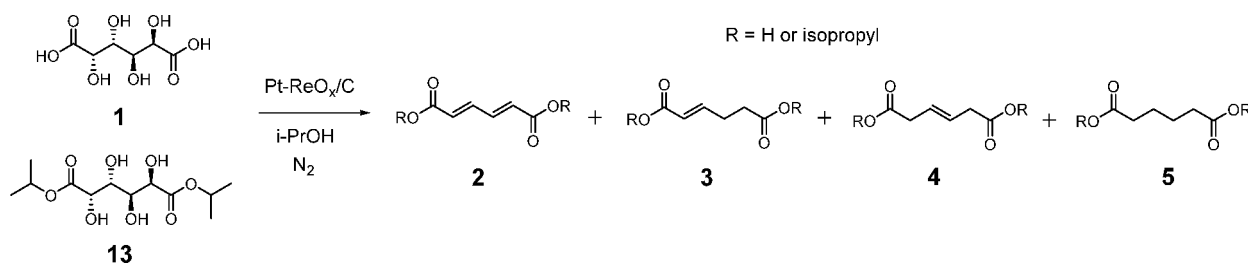
studies of the Pt/C catalyst, prepared from H₂PtCl₆, showed a uniform peak around 200–300 °C, which was accompanied by HCl emission due to the decomposition of Pt^{IV}Cl₆²⁻ and Pt^{II}Cl₄²⁻.^{42,44} Two different peaks at 335 and 417 °C observed in the profile of ReO_x/C indicate the heterogeneous nature of Re on carbon support. The addition of Pt to ReO_x/C resulted in the shift of the first reduction peak to 275 °C in the profile of Pt-ReO_x/C. This shift can be attributed to the hydrogen spillover from metallic Pt to Re.^{43,45} Moreover, the reduction behavior of Pt-ReO_x/C catalyst starts at a lower temperature (125 °C) in comparison to ReO_x/C (200 °C). Shifts in both the reduction peak and the reduction starting temperature exhibit the close interaction between Pt and Re in the Pt-ReO_x/C catalyst, which is consistent with STEM and EDX analysis.

The as-prepared Pt-ReO_x/C has both high-valent Re and metallic Pt, as evidenced by XPS (Figure 4a,b and Table S5). In the curve-fitted results of the Re 4f spectrum, the major oxidation states at binding energies of 44.7 and 47.1 eV represent Re^{VII} (72%), followed by Re^{IV} (27%) and a very small amount of metallic Re⁰ (1%). Pt consists of 85% metallic Pt⁰ with a 4f_{7/2} peak at 71.8 eV and 15% Pt^{II}. The reported binding energy for the Pt 4f_{7/2} peak of bulk metallic Pt⁰ ranged between 71.0 and 71.3 eV.⁴⁶ The shift toward higher binding energy indicates smaller size and high dispersity of Pt particles.^{46,47} The thermal treatment step under N₂ at 480 °C during synthesis results in Pt^{IV} precursor reduction to metallic Pt⁰ due to the reductive properties of the carbon support.⁴⁸ Similar oxidation states of Pt and Re were observed in monometallic Pt/C and ReO_x/C samples (Figure S10 and Table S5).

XRD patterns of bare activated carbon, ReO_x/C, Pt/C, and Pt-ReO_x/C are shown in Figure 3f. Pt⁰ and Re^{VII}, major species detected by XPS analysis, did not appear in the XRD patterns, suggesting a high dispersion of particles in Pt/C and Pt-ReO_x/C. This is consistent with the XPS analysis: the higher Pt⁰ 4f_{7/2} peak position of the catalysts in comparison to that of bulk Pt. While the particles are small and well-dispersed, ReO₂ peaks in the pattern of ReO_x/C and Pt-ReO_x/C suggest the existence of larger particles containing the ReO₂ phase.

3.4. Proposed Reaction Mechanism. As discussed in Bifunctional Catalysis, ReO_x/C was active for DODH but

Table 3. Effect of Concentration of Reaction Solution^a



entry	substrate	concn (M)	convers ^b (%)	product selectivity (%) ^b			
				2	3 and 4	5	others
1 ^c	1	0.025	95	0	0	89	11
2	1	0.1	100	0	2	77	21
3	1	0.25	100	0	5	65	30
4 ^d	13	0.25	90	0	0	83	17

^aReaction conditions unless specified otherwise: 170 °C, 24 h, Pt-ReO_x/C (3.6 mol % Re and 1.4 mol % Pt relative to substrate), *i*-PrOH (10 mL), N₂ (15 bar). ^bConversion and selectivity were calculated by ¹H NMR. ^c*i*-PrOH (40 mL). ^d12 h reaction.

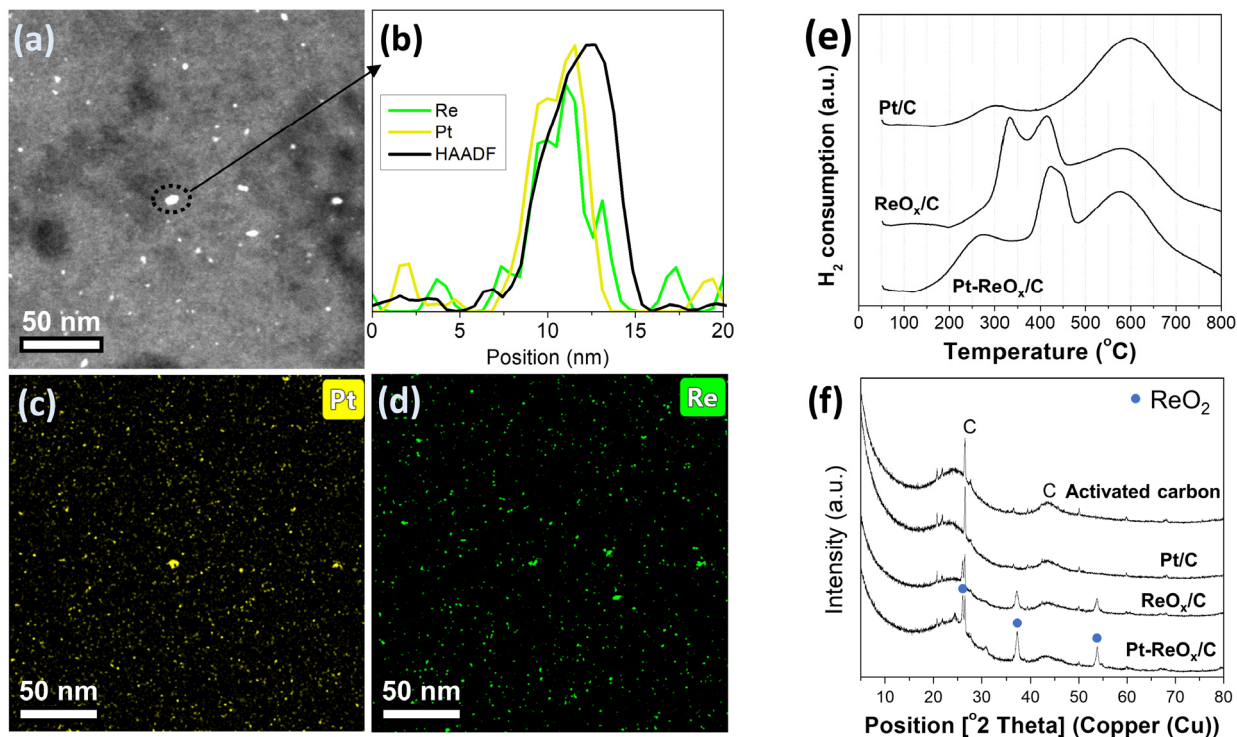


Figure 3. Characterization of as-prepared Pt-ReO_x/C catalyst. (a) STEM high-angle annular dark-field (HAADF) analysis. (b) Line scan elemental analysis on a particle in (a). (c) EDX mapping of Pt. (d) EDX mapping of Re. Analyses of more particles are given in Figure S9. (e) TPR profiles for Pt/C, ReO_x/C, and as-prepared Pt-ReO_x/C. (f) XRD diffractograms of activated carbon, Pt/C, ReO_x/C, and as-prepared Pt-ReO_x/C. Peaks with blue circles at 26, 37, and 54° represent ReO₂.

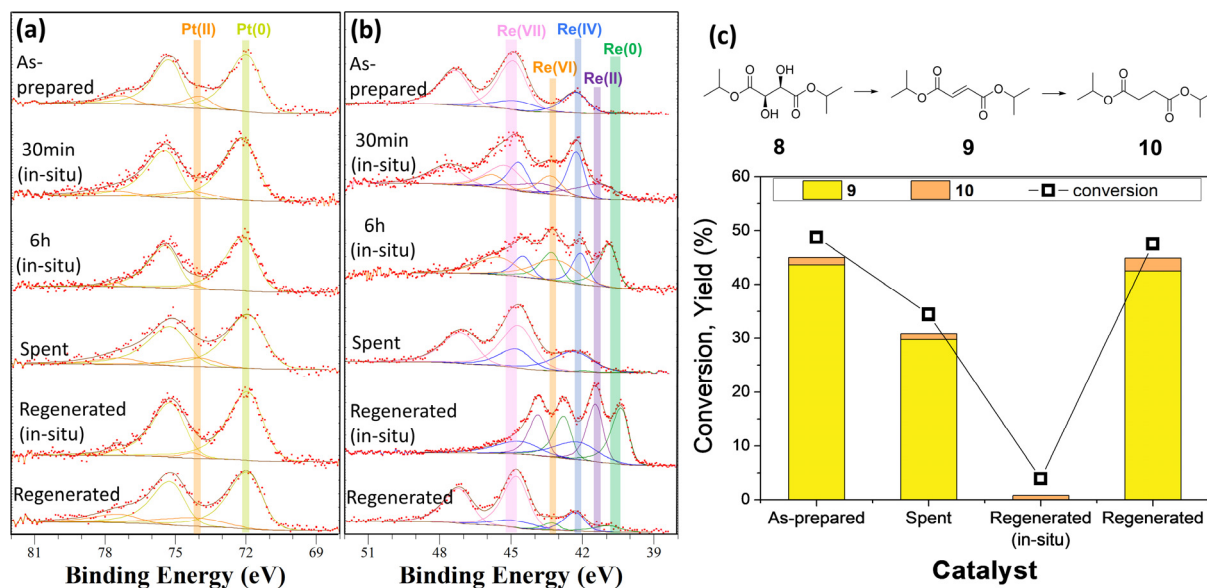


Figure 4. Changes in XPS spectra of (a) Pt 4f and (b) Re 4f in Pt-ReO_x/C over reaction and regeneration. In situ 30 min and 6 h samples under the general reaction conditions for mucic acid (1) conversion were prepared without air exposure. After 6 h of the reaction, the catalyst was separated and washed under atmospheric conditions, followed by drying overnight at 120 °C (spent sample). The spent sample was regenerated at 230 °C under H₂ and transferred to a glovebox without air exposure (in situ regenerated sample). This in situ sample was exposed to air and reoxidized at 120 °C (regenerated sample). (c) Activity test of as-prepared, spent, in situ regenerated, and regenerated samples using diisopropyl L-(+)-tartarate (8) as a substrate. Reaction conditions: 8 (0.5 mmol), catalyst (20 mg), isopropanol (10 mL), N₂ (15 bar), 170 °C, 20 min. The reaction with the in situ regenerated sample was carried out under inert conditions.

inactive for CTH at 170 °C. The addition of Pt to ReO_x/C showed a significant increase in CTH. These, in combination with no activity of Pt/C for DODH, suggest a bifunctional mechanism; DODH occurs on ReO_x and CTH on Pt in the Pt-

ReO_x/C catalyst. The reactivity of a physical mixture of ReO_x/C and Pt/C for the DODH-CTH reaction being similar to that for Pt-ReO_x/C supports the bifunctional mechanism (entry 10 in Table 2).

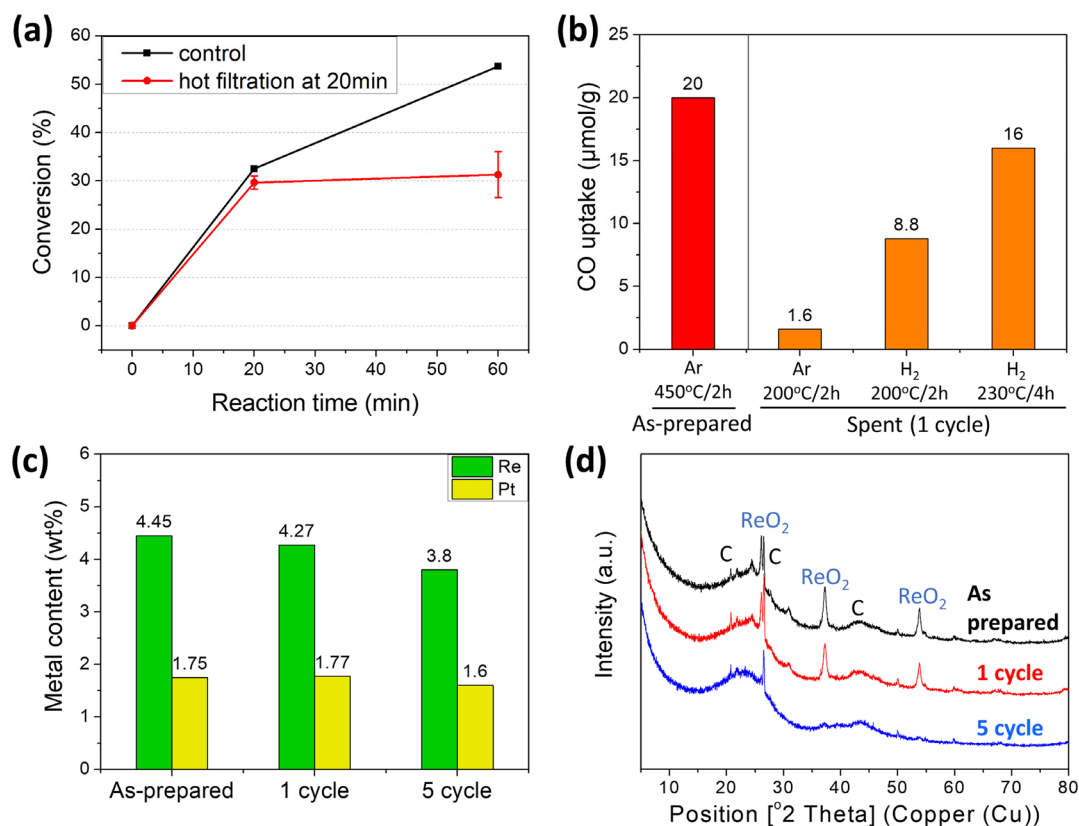
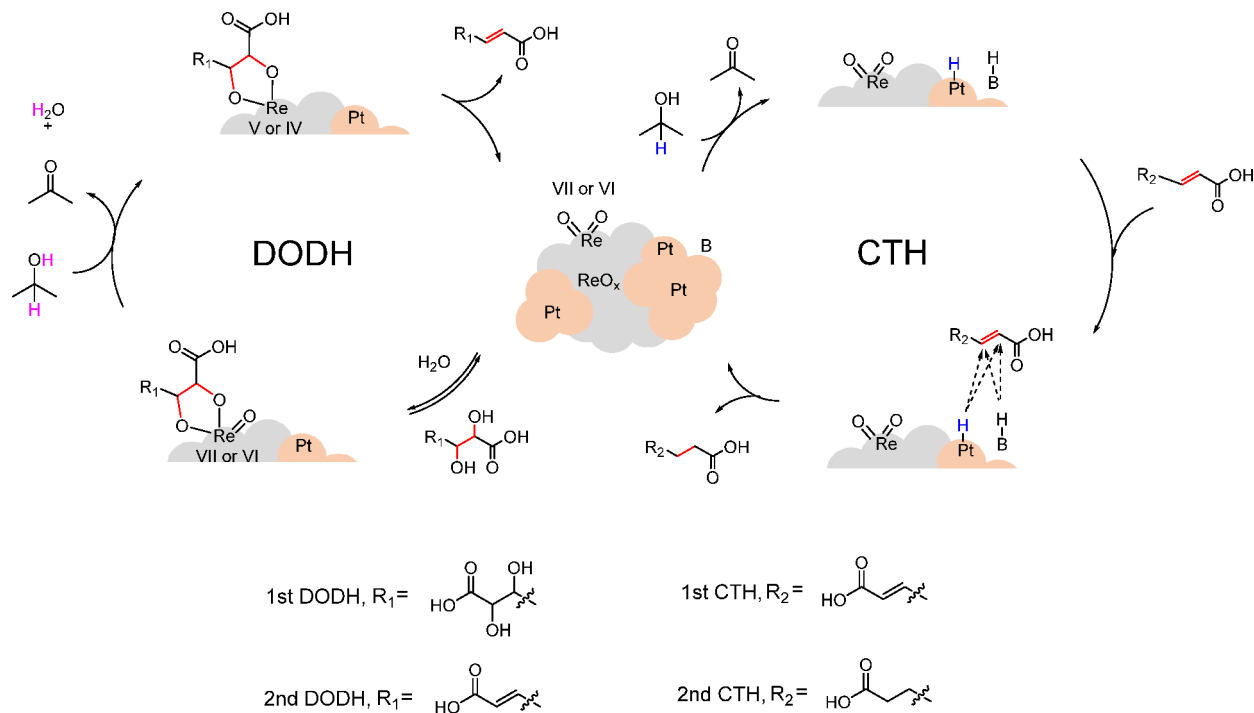


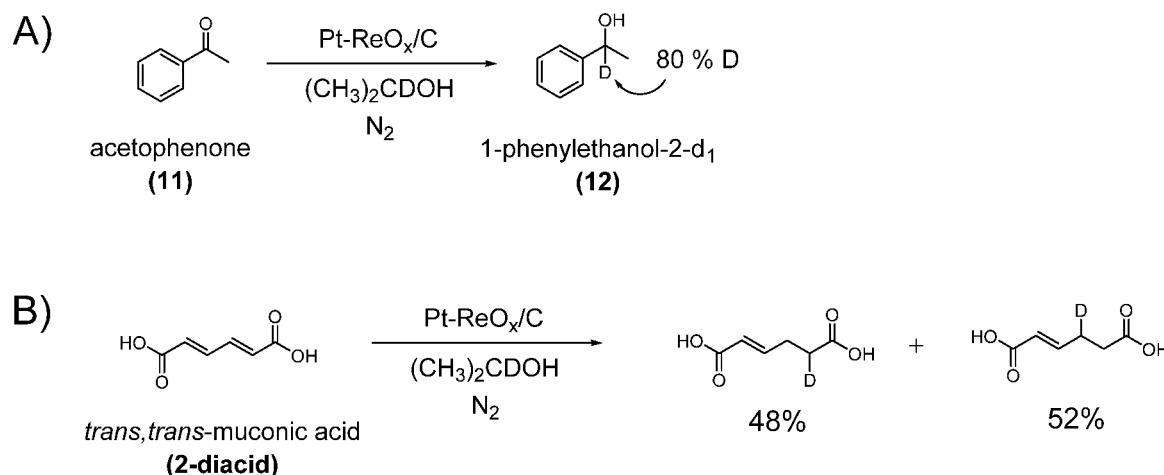
Figure 5. (a) Hot filtration test of the Pt-ReO_x/C catalyst. For the control test, two samples were collected at 20 and 60 min. For the hot filtration test, the reaction solution was extracted from a pressure reactor equipped with a ceramic filtration system at 170 °C after 20 min reaction. The filtrate was submitted to the same reaction conditions for an additional 40 min. Reaction conditions: 8 (4 mmol), Pt-ReO_x/C (100 mg), isopropanol (40 mL), N₂ (15 bar), 170 °C, 20 min. (b) Cumulative CO uptake (μmol/g) on the as-prepared and spent (one cycle) Pt-ReO_x/C with different pretreatment conditions. (c) ICP analysis and (d) XRD spectra of Pt-ReO_x/C for the recycling test.

Scheme 2. Proposed Bifunctional Mechanism for DODH-CTH Tandem Reaction of 1^a



^aB denotes a basic site.

Scheme 3. Isotope Labeling Experiments for CTH of (A) Acetophenone (11) and (B) *trans,trans*-Muconic Acid (2-diacid) with Isopropanol-2-*d*₁^a



^aReaction conditions: substrate (0.5 mmol), Pt-ReO_x/C (15 mg, 4.5 wt % Re, 1.8 wt % Pt), *i*-PrOH-2-*d*₁ (1 mL), N₂ (15 bar), 150 °C, 6 h.

To identify the active species of DODH and CTH, the changes in oxidation states of Re and Pt during the reaction were investigated. Under the general reaction conditions for mucic acid conversion, the oxidation states of Re and Pt were gradually reduced over the course of the reaction, as shown in Figure 4 (see also Table S5). To avoid oxidation of Re during the preparation of samples for XPS, the catalyst after a 30 min or 6 h reaction was separated and transferred to the XPS chamber without exposure to ambient atmosphere. In 30 min, a significant amount of Re^{VII} in the as-prepared sample was reduced with the appearance of Re^{VI} (4f_{7/2} peak at 43.3 eV) and Re^{II} (4f_{7/2} peak at 41.2 eV). Re in the in situ 30 min sample consisted of Re^{VII} (31%), Re^{VI} (16%), Re^{IV} (28%), and Re^{II} (25%). Further reduction of Re proceeded over 6 h, making Re^{VI} (42%), Re^{IV} (23%), and metallic Re⁰ (35%). The reaction profile in Figure 2 shows that the catalysts with the reduced Re oxidation states also converted mucic acid through DODH. It should be noted that DODH of the in situ regenerated sample containing metallic Re⁰ and Re^{II} as the dominant species is shown to be inactive later in this work (Figure 4c). These observations indicate that high oxidation states of ReO_x (Re^{VII}, Re^{VI}, and Re^{IV}) are the species involved in the DODH reaction. This is consistent with previously suggested DODH mechanisms including Re^{VII}/Re^V or Re^{VI}/Re^{IV} redox couples over heterogeneous ReO_x-based catalysts.^{33,35,36,49,50} Similarly, the reduction of Pt under the reaction conditions resulted in 96% of metallic Pt⁰ and a small amount of Pt^{II} (4%) after 6 h of reaction, indicating metallic Pt⁰ as being the active species for CTH.

The reported DODH mechanism involves three steps: formation of Re-diolate, reduction of Re species, and extrusion of olefin.^{14,11,26,33,36,51–53} In the literature on heterogeneous DODH catalysts, oxorhenium species in a nanocluster can be the active species for DODH,^{33,35} while other authors demonstrated isolated ReO_x as the active species.^{49,50} Hot filtration experiments were performed to investigate the contribution of molecular species to the DODH reaction (Figure 5a). After hot filtration at approximately 30% conversion at 170 °C, an additional reaction with the filtrate without the solid catalyst showed a negligible increase in the conversion. The amount of leached Pt and Re in the hot filtration solution is similar to that of the control test solution

filtered at room temperature after 20 min of reaction (2–3% Re and 0.4–0.5% Pt of the original amount of metal added). These results suggest that DODH proceeds mostly on the heterogeneous surface, precluding the involvement of the molecular species.^{33,35} Re^{VII} and Re^{VI}, designated as the active species of DODH in the solid Pt-ReO_x/C catalyst, form Re-diolate by coordinating to 1 (Scheme 2). Isopropanol reduces the rhenium diolato complex, affording acetone as a byproduct (Table S4). The reduced oxorhenium diolate releases an alkene (the reverse of a 3 + 2 dihydroxylation), closing the catalytic cycle on rhenium. After the DODH cycle, the reduced Re goes back to Re^{VII} or Re^{VI}. Two DODH cycles afford 2 from 1.

With regard to the mechanism of CTH over Pt, isotope labeling experiments were conducted. Previously, both a “monohydride mechanism” and “dihydride mechanism” have been proposed for transition-metal-catalyzed CTH (Scheme S2).^{54,55} A deuterium labeling experiment of acetophenone (11) using deuterated isopropanol is a widely used method to distinguish between the two possible CTH mechanisms.^{56,57} Pt-ReO_x/C-catalyzed CTH of 11 with isopropanol-2-*d*₁ showed 80% incorporation of deuterium at the α-C (Scheme 3A and Figure S11). This is indicative of a monohydride mechanism. Only the α-H of the donor forms Pt–H, and this hydride is transferred to the α-C of acetophenone exclusively while the O–H hydrogen ends up on the carbonyl oxygen (Scheme S2).⁵⁸ However, CTH of 2-diacid with isopropanol-2-*d*₁ resulted in the incorporation of deuterium at both α-C and at β-C of the molecule (Scheme 3B and Figure S12). This indicates that the hydride (Pt–H) generated by the monohydride mechanism can be transferred to both α-C and β-C of 2-diacid (Scheme 2). Similarly, incorporation of metal monohydride at α-C and β-C without regioselectivity was observed in the literature in the hydrogenation of α,β-unsaturated carboxylic acid.^{59,60} Moreover, it has been shown that noble-metal heterogeneous catalysts with a base additive transfer hydrogen from isopropanol to ketone or olefin through a monohydride mechanism.^{28,61} In Pt-ReO_x/C, the base sites of the catalyst would act as the base additive, transferring the O–H hydrogen in isopropanol to the olefin (Scheme 2). The possible basic sites include basic sites of the activated carbon support and different Pt species.⁶² It is reported that the basic

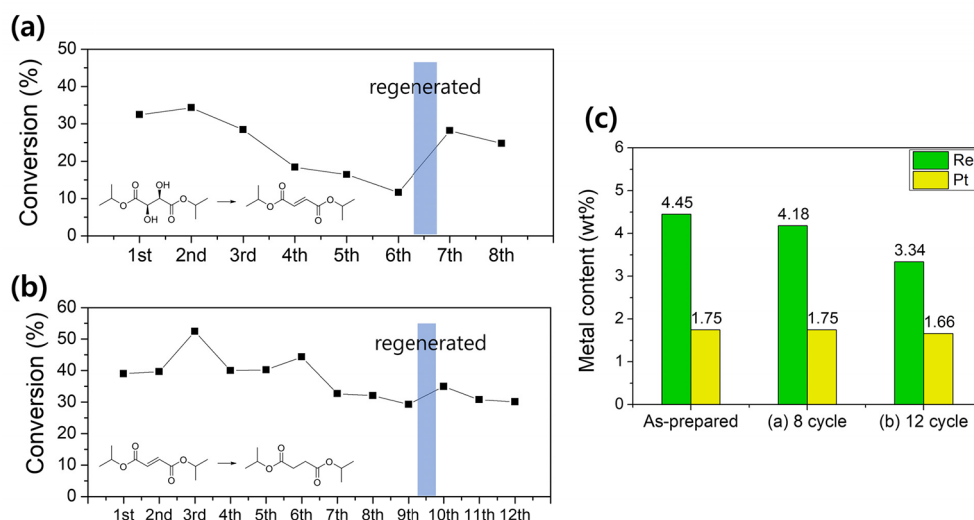


Figure 6. Stability of Pt-ReO_x/C for (a) DODH (8 to 9) and (b) CTH (9 to 10). Reaction conditions: substrate (4 mmol), Pt-ReO_x/C (100 mg), activated carbon (200 mg), isopropanol (40 mL), N₂ (15 bar), 170 °C, 20 min. (c) ICP analysis of as-prepared Pt-ReO_x/C, spent sample after 8 cycles in (a) and 12 cycles in (b). Regeneration conditions: 5% H₂ in Ar, 230 °C, and 4 h, followed by reoxidation (air/120 °C/1 h).

sites of a support material play a role similar to that of base additives in the CTH reaction.⁶³ More details about the basic sites of Pt-ReO_x/C catalyst for CTH reaction will be clarified in our future work.

3.5. Catalyst Recycling and Regeneration. One of the main advantages of heterogeneous catalysts is the possibility of their reuse.⁶⁴ While supported ReO_x catalysts tend to deactivate due to leaching under DODH reaction conditions,^{15,34} some stable and reusable solid ReO_x catalysts have been reported.^{16,33,35} The reusability of the Pt-ReO_x/C catalyst was investigated. The recovered catalyst was tested with new substrate 1 and isopropanol. A lower conversion and selectivity of 5 were observed (entry 2 in Table 2). However, ICP analysis of the catalyst after one cycle showed a small leaching of Re (4% of the original amount of Re added) and no leaching of Pt (Figure 5c). Thus, active site loss into solution during the reaction did not make a major contribution to the loss of activity and selectivity of 5. This, as well as hot filtration experiments, is a significant point in demonstrating that the active catalyst is indeed heterogeneous and not homogeneous from leaching. According to CO chemisorption data, the strongly reduced CO uptake on the spent sample (1.6 μmol/g) was compared to the value for the as-prepared catalyst (20 μmol/g, Figure 5b). These observations suggest that organic deposits during the reaction result in deactivation and lower activity and selectivity. Unidentified byproducts (5–15%) might be responsible for the organic deposits. It is not uncommon for heavy byproducts to form a carbonaceous deposit on the surface of catalysts in the reactions of organic compounds.⁶⁵

To recover reactivity, the spent catalyst was regenerated under an H₂ atmosphere.⁶⁶ The regeneration temperature was chosen to remove the organic deposits on the catalysts and to minimize methanation of the support. With regeneration at 230 °C, the CO uptake of Pt-ReO_x/C was restored to 16 μmol/g, which is a clear indication of the removal of organic deposits from the surfaces of the spent catalyst (Figure 5b). A lower temperature H₂ treatment (200 °C) did not remove organic deposits effectively. The changes in the oxidation states and the activity of Pt-ReO_x/C over the regeneration step are

analyzed in Figure 4 and Table S5. Diisopropyl L-(+)-tartarate (8) was used as a substrate to study the activity of the catalysts for DODH. While the spent catalyst exhibited oxidation states similar to those of the as-prepared Pt-ReO_x/C catalyst, it showed the reduced conversion of 8 due to the organic deposits. During the regeneration step at 230 °C, high oxidation states of ReO_x in the spent sample were reduced to metallic Re⁰ and Re^{II}, as measured by in situ sampling and analysis without exposure to air (in situ regenerated sample). This is consistent with the low reduction starting temperature (125 °C) in TPR spectra of Pt-ReO_x/C (Figure 3e) and XPS results of the reduced Pt-Re bimetallic catalysts in previous reports.^{22,23} The negligible activity of the in situ regenerated sample indicates that the low oxidation states of Re are not active for DODH, in agreement with previous observations.^{33,49} The in situ regenerated sample was reoxidized by exposure to air and drying at 120 °C for 1 h (regenerated sample). The regenerated sample showed oxidation states and activity for DODH similar to those of the as-prepared catalyst, confirming that the regeneration at 230 °C effectively removes the organic deposits. It should also be highlighted that the reoxidation step is necessary after the regeneration to recover high oxidation states of Re and reactivity for DODH.

The regeneration and reoxidation were employed with the catalyst after the second run in Table 2. After regeneration at 230 °C for 2 h and reoxidation, the reactivity of Pt-ReO_x/C for the conversion of 1 was regained in the subsequent third and fourth runs (entries 3 and 4 in Table 2). A longer regeneration time (4 h) under H₂ at 230 °C resulted in a similar performance of the as-prepared catalyst (Table 2, entry 5). Over the course of five sequential reactions with the same catalyst sample, some Re and Pt was leached out; however, this did not affect the yield of 5 at high conversion (Figure 5c). It has been addressed that the recycling test with a single measurement at high conversion in a batch reaction system might not fully reflect the deactivation of the catalyst.^{67,68} Thus, the catalyst stability should be tested at kinetically controlled conversion, which is shown later in this work. On the basis of XPS and XRD analysis, the Pt-ReO_x/C catalyst maintained its oxidation states and was still well-dispersed after

Table 4. Substrate Scope of DODH-CTH Tandem Reaction of Sugar Acids and Alcohols over Pt-ReO_x/C^a

Entry	Substrate	Reaction condition	Product (% yield) ^b
1	 1	170 °C 24 h	 5 (85%)
2	 13	170 °C 6 h	 5-diester (90%)
3 ^c	 14	170 °C 24 h	 15 (41%) 5 (15%)
4	 16	170 °C 6 h	 17 (98%)
5	 18	170 °C 6 h	 19 (87%)
6	 20	200 °C 24 h	 21 (18%)^[d] 22 (19%)^d

^aReaction conditions unless specified otherwise: Pt-ReO_x/C (150 mg, 4.5 wt % Re, 1.8 wt % Pt), substrate (1.0 mmol), *i*-PrOH (40 mL), and N₂ (15 bar). ^bCalculated by ¹H NMR. ^cSubstrate (0.5 mmol). ^dCalculated by GC-FID.

multiple recycling tests (Figure 5d and Figure S14). After five consecutive cycles, ReO₂ peaks disappeared, possibly due to a change to an amorphous phase over multiple reactions and regenerations.

Interestingly, in comparison to the bifunctional bimetallic Pt-ReO_x/C catalyst, the physical mixture of Pt/C and ReO_x/C could not be regenerated. Much lower conversions in the second and third cycles were observed (entry 11 in Table 2 and Figure S13). The recycled physical mixture after regeneration exhibited similar oxidation states and metal amounts but lower CO uptake in comparison to as-prepared catalysts (Figure S14 and Tables S6 and S7). Thus, the lower conversion is attributed to organic deposits on ReO_x/C that

were not removed during regeneration. In the physical mixture, ReO_x alone might not uptake enough hydrogen to eliminate organic deposits. In contrast, in Pt-ReO_x/C, hydrogen spillover from Pt enhances the regeneration of ReO_x sites.^{47,69–71} Thus, while the Pt-ReO_x interface was not critical for the bifunctional DODH/CTH reaction, it was critical for effective regeneration of the catalyst.

3.6. Stability Test. The stability of Pt-ReO_x/C was studied by observing changes in its activity for DODH and CTH at low conversion levels over multiple consecutive runs. The first run for the conversion of **8** with Pt-ReO_x/C showed 33% conversion after 20 min of reaction at 170 °C, producing **9** as a major product through DODH (Figure 6a). The conversion

gradually decreased until the sixth cycle, where the conversion was 12%. This deactivation was attributed to both organic deposits on ReO_x and active site leaching. The regeneration including reoxidation increased the conversion up to 28% in the seventh cycle, indicating organic deposits making a major contribution to the observed deactivation in the first six cycles. The 4% difference between the first and seventh cycle can be explained by the leaching of Re over the multiple runs. ICP analysis of the catalyst after eight cycles showed some leaching of Re, attributed to the slightly reduced conversion of the regenerated catalyst in comparison to the as-prepared catalyst (Figure 6c). While ReO_x in the Pt- ReO_x/C catalyst can be deactivated by both fouling and leaching during the DODH-CTH reaction, the amount of Re leached out from the catalyst is small (Figures 5c and 6c). As a result, the catalyst could be reusable several times after regeneration without significantly reduced reactivity.

Interestingly, the activity of Pt sites for CTH did not change much (Figure 6b). Over 12 consecutive runs, the conversion of **9** was slightly reduced from 40% to 30% and maintained at around 30% even with regeneration. The results indicate that deactivation by organic deposits on Pt sites is negligible and a small leaching of Pt sites could be a reason for the reduced conversion (Figure 6c). Loss of Re over the 12 runs in Figure 6b is more pronounced than that over 8 runs in Figure 6a. This is probably because the organic deposits on ReO_x in Figure 6a inhibit the leaching of Re.

The leaching of rhenium species from solid $\text{ReO}_x/\text{support}$ catalysts in the DODH reaction was studied in detail by Jentoft et al.¹⁵ The proposed leaching mechanism during DODH reaction formed a rhenium diolate by chelating the surface rhenium with olefin or diol as a chelating ligand. The extent of leaching depended on the solubility of the resulting rhenium diolate complexes in the solvent. The leached rhenium-diolate species were characterized by UV-vis spectroscopy, exhibiting a peak at 493–499 nm while the perrhenate absorption was around 230 nm.¹⁵ To investigate the rhenium species leached from the Pt- ReO_x/C catalyst, DODH of (*R,R*)-(+)-hydrobenzoin was conducted and the supernatant was analyzed by UV-vis and NMR spectroscopy. UV-vis spectra of the supernatant showed a peak at around 507 nm, indicating the possibility of rhenium-diolate as a leached complex (Figure S16). This possibility was confirmed by ¹H NMR results of the supernatant. A broad peak at 5.62 ppm might be assigned to the diolato ring protons (Figure S17b). MTO-catalyzed DODH of (*R,R*)-(+)-hydrobenzoin formed MTO-diolate, $\text{MeRe}^{\text{VII}}(\text{OCHPhCHPhO})$, characterized by ¹H NMR (Figure S17a) and our previous study.⁵² The MTO-diolate shows a broad peak of the diolato ring protons at 5.75 ppm and a $\text{Re}-\text{CH}_3$ peak at 2.7 ppm. In addition, the MTO-diolate exhibited a peak at around 476 nm in UV-vis spectra (Figure S16). The different peak positions in NMR and UV-vis spectra might be due to the different structures between MTO-diolate and the rhenium diolate leached from Pt- ReO_x/C . These results suggest a rhenium-diolate intermediate as a possible leached rhenium species. As addressed in previous studies, leaching by chelation with the reactant and product can be mitigated by choosing (1) an appropriate solvent that reduces the solubility of rhenium-diolate species and (2) a different support material that enhances the metal-support interaction.^{15,35}

3.7. Substrate Scope. To explore the substrate scope for Pt- ReO_x/C , we studied various diols (Table 4). Diisopropyl mucate (**13**) was converted to **5-diester** in high yield (90%).

This indicates that the conversion of **1** is hampered by competition between DODH and esterification. *D*-Glucaric acid lactone can be used as a substrate to produce **5**.^{5,16} The conversion of *D*-glucaric-1,4-lactone (**14**) through DODH-CTH over Pt- ReO_x/C gave 41% of **15** and 15% of **5**. Ring opening of **15** is required to increase yields of **5**. In addition to C6 sugar acids, the bifunctional catalyst successfully converted *L*-(+)-tartaric acid (**16**), a C4 sugar acid, to a 98% yield of succinic acid and its esters (**17**). The same reaction was also applied to sugar alcohols. Glycerol (**18**) was converted to 1-propanol (**19**) in 87% yield. *D*-Sorbitol (**20**) contains six OH groups; thus, three DODH-CTH cycles produced *n*-hexane (**22**). All of the NMR and GC spectra of the reaction solution in this section are shown in Figures S18–S23.

4. CONCLUSION

Bifunctional Pt- ReO_x/C catalysts were prepared and shown to produce adipates **5** from the sugar diacid **1** through tandem DODH-CTH reactions in high yield (77% isolated adipic acid). Evidence was provided that the oxorhenium(VI and VII) sites are responsible for DODH. The metallic Pt⁰ sites in Pt- ReO_x/C significantly enhanced the selectivity of adipates **5** through CTH without affecting DODH, as long as the Pt loading was maintained at or below 1.8 wt %. Isopropanol works as a hydrogen donor as well as a solvent for both DODH and CTH. Reusability and stability tests of the Pt- ReO_x/C catalyst indicate catalyst deactivation mostly due to organic material deposition that can be removed by regeneration with H_2 . With the regeneration and reoxidation steps, the recycled Pt- ReO_x/C catalyst afforded similar conversion and selectivity of adipates up to five cycles in a 6 h reaction, where the conversion is high (70–80%). However, in the recycling tests at moderate conversion (30–40%), the conversion of diol was not fully recovered with the regeneration and reoxidation due to some rhenium leaching. Furthermore, DODH-CTH over the bimetallic catalyst removed hydroxyl groups in various sugar acids and alcohols. A bifunctional mechanism was proposed on the basis of the reactivity with various substrates, spectroscopic analysis, and isotope labeling experiments.

■ ASSOCIATED CONTENT

Supporting Information

The Supporting Information is available free of charge at <https://pubs.acs.org/doi/10.1021/acscatal.0c04158>.

Catalyst screening, optimal reaction conditions, isolation of adipic acid, isotope labeling experiment, carbon balance, GC-TCD of the gas phase, characterization of the leached rhenium species, NMR spectra of the DODH-CTH reaction with various substrates, and additional characterization data including STEM-EDX and TEM images, XPS spectra, CO chemisorption, and FT-IR spectra of pyridine of as-prepared, spent, regenerated, and reduced Pt- ReO_x/C (PDF)

■ AUTHOR INFORMATION

Corresponding Author

Mahdi M. Abu-Omar – Department of Chemical Engineering and Department of Chemistry and Biochemistry, University of California Santa Barbara, Santa Barbara, California 93106, United States; orcid.org/0000-0002-4412-1985; Email: abuomar@chem.ucsb.edu

Authors

Jun Hee Jang – Department of Chemical Engineering, University of California Santa Barbara, Santa Barbara, California 93106, United States; orcid.org/0000-0002-1879-0544

Insoo Ro – Department of Chemical Engineering, University of California Santa Barbara, Santa Barbara, California 93106, United States; Department of Chemical and Biomolecular Engineering, Seoul National University of Science and Technology, Seoul 01811, Republic of Korea; orcid.org/0000-0002-4704-142X

Phillip Christopher – Department of Chemical Engineering, University of California Santa Barbara, Santa Barbara, California 93106, United States; orcid.org/0000-0002-4898-5510

Complete contact information is available at:
<https://pubs.acs.org/10.1021/acscatal.0c04158>

Notes

The authors declare no competing financial interest.

ACKNOWLEDGMENTS

This work was supported by the US Department of Energy, Office of Science, Basic Energy Science, Award No. DE-SC0019161 (M.M.A.-O.). The use of STEM, XRD, XPS, and ICP equipment in the UCSB MRL was supported by the MRSEC Program of the National Science Foundation under Award No. DMR 1720256. Fan Zhang and Ali Chamas are acknowledged for gas product analysis. We thank Jordan Finzel for discussions on CO chemisorption data.

REFERENCES

- (1) Rinaldi, R.; Jastrzebski, R.; Clough, M. T.; Ralph, J.; Kennema, M.; Buijtinckx, P. C. A.; Weckhuysen, B. M. Paving the Way for Lignin Valorisation: Recent Advances in Bioengineering, Biorefining and Catalysis. *Angew. Chem., Int. Ed.* **2016**, *55* (29), 8164–8215.
- (2) Lin, Y.-C.; Huber, G. W. The Critical Role of Heterogeneous Catalysis in Lignocellulosic Biomass Conversion. *Energy Environ. Sci.* **2009**, *2* (1), 68–80.
- (3) Straathof, A. J. J.; Bampouli, A. Potential of Commodity Chemicals to Become Bio-based According to Maximum Yields and Petrochemical Prices. *Biofuels, Bioprod. Biorefin.* **2017**, *11* (5), 798–810.
- (4) Veski, R.; Veski, S. Aliphatic Dicarboxylic Acids from Oil Shale Organic Matter - Historic Review. *Oil Shale* **2019**, *36* (1), 76.
- (5) Larson, R. T.; Samant, A.; Chen, J.; Lee, W.; Bohn, M. A.; Ohlmann, D. M.; Zuend, S. J.; Toste, F. D. Hydrogen Gas-Mediated Deoxydehydration/Hydrogenation of Sugar Acids: Catalytic Conversion of Glucarates to Adipates. *J. Am. Chem. Soc.* **2017**, *139* (40), 14001–14004.
- (6) Draths, K. M.; Frost, J. W. Environmentally Compatible Synthesis of Adipic Acid from D-Glucose. *J. Am. Chem. Soc.* **1994**, *116* (1), 399–400.
- (7) Niu, W.; Draths, K. M.; Frost, J. W. Benzene-Free Synthesis of Adipic Acid. *Biotechnol. Prog.* **2002**, *18* (2), 201–211.
- (8) Boussie, T. R.; Dias, E. L.; Fresco, Z. M.; Murphy, V. J.; Shoemaker, J.; Archer, R.; Jiang, H. Production of Adipic Acid and Derivatives from Carbohydrate-Containing Materials. US 8669397B2, March 11, 2014.
- (9) Gilkey, M. J.; Mironenko, A. V.; Vlachos, D. G.; Xu, B. Adipic Acid Production via Metal-Free Selective Hydrogenolysis of Biomass-Derived Tetrahydrofuran-2,5-Dicarboxylic Acid. *ACS Catal.* **2017**, *7* (10), 6619–6634.
- (10) Wei, L.; Zhang, J.; Deng, W.; Xie, S.; Zhang, Q.; Wang, Y. Catalytic Transformation of 2,5-Furandicarboxylic Acid to Adipic Acid over Niobic Acid-Supported Pt Nanoparticles. *Chem. Commun.* **2019**, *55* (55), 8013–8016.
- (11) Li, X.; Wu, D.; Lu, T.; Yi, G.; Su, H.; Zhang, Y. Highly Efficient Chemical Process to Convert Mucic Acid into Adipic Acid and DFT Studies of the Mechanism of the Rhenium-Catalyzed Deoxydehydration. *Angew. Chem., Int. Ed.* **2014**, *53* (16), 4200–4204.
- (12) Tshibalonza, N. N.; Monbaliu, J.-C. M. The Deoxydehydration (DODH) Reaction: A Versatile Technology for Accessing Olefins from Bio-Based Polyols. *Green Chem.* **2020**, *22* (15), 4801–4848.
- (13) Dethlefsen, J. R.; Fristrup, P. Rhenium-Catalyzed Deoxydehydration of Diols and Polyols. *ChemSusChem* **2015**, *8* (5), 767–775.
- (14) Shiramizu, M.; Toste, F. D. Expanding the Scope of Biomass-Derived Chemicals through Tandem Reactions Based on Oxorhenium-Catalyzed Deoxydehydration. *Angew. Chem., Int. Ed.* **2013**, *52* (49), 12905–12909.
- (15) Sharkey, B. E.; Jentoft, F. C. Fundamental Insights into Deactivation by Leaching during Rhenium-Catalyzed Deoxydehydration. *ACS Catal.* **2019**, *9* (12), 11317–11328.
- (16) Lin, J.; Song, H.; Shen, X.; Wang, B.; Xie, S.; Deng, W.; Wu, D.; Zhang, Q.; Wang, Y. Zirconia-Supported Rhenium Oxide as an Efficient Catalyst for the Synthesis of Biomass-Based Adipic Acid Ester. *Chem. Commun.* **2019**, *55* (74), 11017–11020.
- (17) Wei, Z.; Sun, J.; Li, Y.; Dartye, A. K.; Wang, Y. Bimetallic Catalysts for Hydrogen Generation. *Chem. Soc. Rev.* **2012**, *41* (24), 7994–8008.
- (18) Carter, J. L.; McVinker, G. B.; Weissman, W.; Kmak, M. S.; Sinfelt, J. H. Bimetallic Catalysts; Application in Catalytic Reforming. *Appl. Catal.* **1982**, *3* (4), 327–346.
- (19) Barbier, J. Deactivation of Reforming Catalysts by Coking - a Review. *Appl. Catal.* **1986**, *23* (2), 225–243.
- (20) Parera, J. Stability of Bimetallic Reforming Catalysts. *J. Catal.* **1988**, *112* (2), 357–365.
- (21) Kunkes, E. L.; Simonetti, D. A.; Dumesic, J. A.; Pyrz, W. D.; Murillo, L. E.; Chen, J. G.; Buttrey, D. J. The Role of Rhenium in the Conversion of Glycerol to Synthesis Gas over Carbon Supported Platinum–Rhenium Catalysts. *J. Catal.* **2008**, *260* (1), 164–177.
- (22) Zhang, L.; Karim, A. M.; Engelhard, M. H.; Wei, Z.; King, D. L.; Wang, Y. Correlation of Pt–Re Surface Properties with Reaction Pathways for the Aqueous-Phase Reforming of Glycerol. *J. Catal.* **2012**, *287*, 37–43.
- (23) Falcone, D. D.; Hack, J. H.; Klyushin, A. Yu.; Knop-Gericke, A.; Schlögl, R.; Davis, R. J. Evidence for the Bifunctional Nature of Pt–Re Catalysts for Selective Glycerol Hydrogenolysis. *ACS Catal.* **2015**, *5* (10), 5679–5695.
- (24) Raju, S.; Moret, M.-E.; Klein Gebbink, R. J. M. Rhenium-Catalyzed Dehydration and Deoxydehydration of Alcohols and Polyols: Opportunities for the Formation of Olefins from Biomass. *ACS Catal.* **2015**, *5* (1), 281–300.
- (25) Dethlefsen, J. R.; Lupp, D.; Teshome, A.; Nielsen, L. B.; Fristrup, P. Molybdenum-Catalyzed Conversion of Diols and Biomass-Derived Polyols to Alkenes Using Isopropyl Alcohol as Reductant and Solvent. *ACS Catal.* **2015**, *5* (6), 3638–3647.
- (26) Shiramizu, M.; Toste, F. D. Deoxygenation of Biomass-Derived Feedstocks: Oxorhenium-Catalyzed Deoxydehydration of Sugars and Sugar Alcohols. *Angew. Chem., Int. Ed.* **2012**, *51* (32), 8082–8086.
- (27) Wang, Y.; Huang, Z.; Leng, X.; Zhu, H.; Liu, G.; Huang, Z. Transfer Hydrogenation of Alkenes Using Ethanol Catalyzed by a NCP Pincer Iridium Complex: Scope and Mechanism. *J. Am. Chem. Soc.* **2018**, *140* (12), 4417–4429.
- (28) Alonso, F.; Riente, P.; Rodríguez-Reinoso, F.; Ruiz-Martínez, J.; Sepúlveda-Escribano, A.; Yus, M. Platinum Nanoparticles Supported on Titania as an Efficient Hydrogen-Transfer Catalyst. *J. Catal.* **2008**, *260* (1), 113–118.
- (29) Johnstone, R. A. W.; Wilby, A. H.; Entwistle, I. D. Heterogeneous Catalytic Transfer Hydrogenation and Its Relation to Other Methods for Reduction of Organic Compounds. *Chem. Rev.* **1985**, *85* (2), 129–170.
- (30) Wang, D.; Astruc, D. The Golden Age of Transfer Hydrogenation. *Chem. Rev.* **2015**, *115* (13), 6621–6686.

- (31) Alonso, F.; Riente, P.; Yus, M. Nickel Nanoparticles in Hydrogen Transfer Reactions. *Acc. Chem. Res.* **2011**, *44* (5), 379–391.
- (32) Yang, G.; Bauer, T. J.; Haller, G. L.; Baráth, E. H-Transfer Reactions of Internal Alkenes with Tertiary Amines as H-Donors on Carbon Supported Noble Metals. *Org. Biomol. Chem.* **2018**, *16* (7), 1172–1177.
- (33) Jang, J. H.; Sohn, H.; Camacho-Bunquin, J.; Yang, D.; Park, C. Y.; Delferro, M.; Abu-Omar, M. M. Deoxydehydration of Biomass-Derived Polyols with a Reusable Unsupported Rhenium Nanoparticles Catalyst. *ACS Sustainable Chem. Eng.* **2019**, *7* (13), 11438–11447.
- (34) Denning, A. L.; Dang, H.; Liu, Z.; Nicholas, K. M.; Jentoft, F. C. Deoxydehydration of Glycols Catalyzed by Carbon-Supported Perrhenate. *ChemCatChem* **2013**, *5* (12), 3567–3570.
- (35) Sandbrink, L.; Klindtworth, E.; Islam, H.-U.; Beale, A. M.; Palkovits, R. $\text{ReO}_x/\text{TiO}_2$: A Recyclable Solid Catalyst for Deoxydehydration. *ACS Catal.* **2016**, *6* (2), 677–680.
- (36) Tazawa, S.; Ota, N.; Tamura, M.; Nakagawa, Y.; Okumura, K.; Tomishige, K. Deoxydehydration with Molecular Hydrogen over Ceria-Supported Rhenium Catalyst with Gold Promoter. *ACS Catal.* **2016**, *6* (10), 6393–6397.
- (37) Ota, N.; Tamura, M.; Nakagawa, Y.; Okumura, K.; Tomishige, K. Hydrodeoxygenation of Vicinal OH Groups over Heterogeneous Rhenium Catalyst Promoted by Palladium and Ceria Support. *Angew. Chem., Int. Ed.* **2015**, *54* (6), 1897–1900.
- (38) Zhang, B.; Qi, Z.; Li, X.; Ji, J.; Zhang, L.; Wang, H.; Liu, X.; Li, C. Cleavage of Lignin C–O Bonds over a Heterogeneous Rhenium Catalyst through Hydrogen Transfer Reactions. *Green Chem.* **2019**, *21* (20), 5556–5564.
- (39) Robinson, A. M.; Hensley, J. E.; Medlin, J. W. Bifunctional Catalysts for Upgrading of Biomass-Derived Oxygenates: A Review. *ACS Catal.* **2016**, *6* (8), 5026–5043.
- (40) Bao, J.; He, J.; Zhang, Y.; Yoneyama, Y.; Tsubaki, N. A Core/Shell Catalyst Produces a Spatially Confined Effect and Shape Selectivity in a Consecutive Reaction. *Angew. Chem., Int. Ed.* **2008**, *47* (2), 353–356.
- (41) Klabunde, J.; Bischoff, C.; Papa, A. J. Propanols. In *Ullmann's Encyclopedia of Industrial Chemistry*; Wiley-VCH: Weinheim, Germany, 2018; pp 1–14.
- (42) Simonetti, D.; Kunkes, E.; Dumesic, J. Gas-Phase Conversion of Glycerol to Synthesis Gas over Carbon-Supported Platinum and Platinum–Rhenium Catalysts. *J. Catal.* **2007**, *247* (2), 298–306.
- (43) Di, X.; et al. Influence of Re–M Interactions in Re–M/C Bimetallic Catalysts Prepared by a Microwave-Assisted Thermolytic Method on Aqueous-Phase Hydrogenation of Succinic Acid. *Catal. Sci. Technol.* **2017**, *7* (22), 5212–5223.
- (44) Fraga, M. A.; Jordão, E.; Mendes, M. J.; Freitas, M. M. A.; Faria, J. L.; Figueiredo, J. L. Properties of Carbon-Supported Platinum Catalysts: Role of Carbon Surface Sites. *J. Catal.* **2002**, *209* (2), 355–364.
- (45) Mieville, R. Platinum–Rhenium Interaction: A Temperature-Programmed Reduction Study. *J. Catal.* **1984**, *87* (2), 437–442.
- (46) Torres, G. C.; Jablonski, E. L.; Baronetti, G. T.; Castro, A. A.; de Miguel, S. R.; Scelza, O. A.; Blanco, M. D.; Peña Jiménez, M. A.; Fierro, J. L. G. Effect of the Carbon Pre-Treatment on the Properties and Performance for Nitrobenzene Hydrogenation of Pt/C Catalysts. *Appl. Catal., A* **1997**, *161* (1–2), 213–226.
- (47) Kuo, C.-T.; Lu, Y.; Kovarik, L.; Engelhard, M.; Karim, A. M. Structure Sensitivity of Acetylene Semi-Hydrogenation on Pt Single Atoms and Subnanometer Clusters. *ACS Catal.* **2019**, *9* (12), 11030–11041.
- (48) de Miguel, S. R.; Scelza, O. A.; Román-Martínez, M. C.; Salinas-Martínez de Lecea, C.; Cazorla-Amorós, D.; Linares-Solano, A. States of Pt in Pt/C Catalyst Precursors after Impregnation, Drying and Reduction Steps. *Appl. Catal., A* **1998**, *170* (1), 93–103.
- (49) Ota, N.; Tamura, M.; Nakagawa, Y.; Okumura, K.; Tomishige, K. Performance, Structure, and Mechanism of ReO_x -Pd/CeO₂ Catalyst for Simultaneous Removal of Vicinal OH Groups with H₂. *ACS Catal.* **2016**, *6* (5), 3213–3226.
- (50) Xi, Y.; Yang, W.; Ammal, S. C.; Lauterbach, J.; Pagan-Torres, Y.; Heyden, A. Mechanistic Study of the Ceria Supported, Re-Catalyzed Deoxydehydration of Vicinal OH Groups. *Catal. Sci. Technol.* **2018**, *8* (22), 5750–5762.
- (51) Yi, J.; Liu, S.; Abu-Omar, M. M. Rhenium-Catalyzed Transfer Hydrogenation and Deoxygenation of Biomass-Derived Polyols to Small and Useful Organics. *ChemSusChem* **2012**, *5* (8), 1401–1404.
- (52) Liu, S.; Senocak, A.; Smeltz, J. L.; Yang, L.; Wegenhart, B.; Yi, J.; Kenttämä, H. I.; Ison, E. A.; Abu-Omar, M. M. Mechanism of MTO-Catalyzed Deoxydehydration of Diols to Alkenes Using Sacrificial Alcohols. *Organometallics* **2013**, *32* (11), 3210–3219.
- (53) Arceo, E.; Ellman, J. A.; Bergman, R. G. Rhenium-Catalyzed Didehydroxylation of Vicinal Diols to Alkenes Using a Simple Alcohol as a Reducing Agent. *J. Am. Chem. Soc.* **2010**, *132* (33), 11408–11409.
- (54) Bäckvall, J.-E. Transition Metal Hydrides as Active Intermediates in Hydrogen Transfer Reactions. *J. Organomet. Chem.* **2002**, *652* (1–2), 105–111.
- (55) Samec, J. S. M.; Bäckvall, J.-E.; Andersson, P. G.; Brandt, P. Mechanistic Aspects of Transition Metal-Catalyzed Hydrogen Transfer Reactions. *Chem. Soc. Rev.* **2006**, *35* (3), 237–248.
- (56) Zhang, G.; Hanson, S. K. Cobalt-Catalyzed Transfer Hydrogenation of C = O and C = N Bonds. *Chem. Commun.* **2013**, *49* (86), 10151–10153.
- (57) Alonso, F.; Riente, P.; Yus, M. Hydrogen-Transfer Reduction of Carbonyl Compounds Promoted by Nickel Nanoparticles. *Tetrahedron* **2008**, *64* (8), 1847–1852.
- (58) Gilkey, M. J.; Xu, B. Heterogeneous Catalytic Transfer Hydrogenation as an Effective Pathway in Biomass Upgrading. *ACS Catal.* **2016**, *6* (3), 1420–1436.
- (59) Brown, J. M.; Parker, D. Mechanism of Asymmetric Homogeneous Hydrogenation. Rhodium-Catalyzed Reductions with Deuterium and Hydrogen Deuteride. *Organometallics* **1982**, *1* (7), 950–956.
- (60) Landis, C. R.; Brauch, T. W. Probing the Nature of H₂ Activation in Catalytic Asymmetric Hydrogenation. *Inorg. Chim. Acta* **1998**, *270* (1–2), 285–297.
- (61) Abarca, B.; Adam, R.; Ballesteros, R. An Efficient One Pot Transfer Hydrogenation and N-Alkylation of Quinolines with Alcohols Mediated by Pd/C/Zn. *Org. Biomol. Chem.* **2012**, *10* (9), 1826–1833.
- (62) Shafeeyan, M. S.; Daud, W. M. A. W.; Houshmand, A.; Shamiri, A. A Review on Surface Modification of Activated Carbon for Carbon Dioxide Adsorption. *J. Anal. Appl. Pyrolysis* **2010**, *89* (2), 143–151.
- (63) Long, J.; Zhou, Y.; Li, Y. Transfer Hydrogenation of Unsaturated Bonds in the Absence of Base Additives Catalyzed by a Cobalt-Based Heterogeneous Catalyst. *Chem. Commun.* **2015**, *51* (12), 2331–2334.
- (64) Dhakshinamoorthy, A.; Asiri, A. M.; Garcia, H. Metal Organic Frameworks as Versatile Hosts of Au Nanoparticles in Heterogeneous Catalysis. *ACS Catal.* **2017**, *7* (4), 2896–2919.
- (65) Goula, M. A.; Lemonidou, A. A.; Efstathiou, A. M. Characterization of Carbonaceous Species Formed during Reforming of CH₄ with CO₂ over Ni/CaO–Al₂O₃ Catalysts Studied by Various Transient Techniques. *J. Catal.* **1996**, *161* (2), 626–640.
- (66) Jae, J.; Zheng, W.; Lobo, R. F.; Vlachos, D. G. Production of Dimethylfuran from Hydroxymethylfurfural through Catalytic Transfer Hydrogenation with Ruthenium Supported on Carbon. *ChemSusChem* **2013**, *6* (7), 1158–1162.
- (67) Sádaba, I.; López Granados, M.; Riisager, A.; Taarning, E. Deactivation of Solid Catalysts in Liquid Media: The Case of Leaching of Active Sites in Biomass Conversion Reactions. *Green Chem.* **2015**, *17* (8), 4133–4145.
- (68) Scott, S. L. A Matter of Life(Time) and Death. *ACS Catal.* **2018**, *8* (9), 8597–8599.
- (69) Conner, W. C.; Falconer, J. L. Spillover in Heterogeneous Catalysis. *Chem. Rev.* **1995**, *95* (3), 759–788.

(70) Ro, I.; Resasco, J.; Christopher, P. Approaches for Understanding and Controlling Interfacial Effects in Oxide-Supported Metal Catalysts. *ACS Catal.* **2018**, *8* (8), 7368–7387.

(71) Ro, I.; Xu, M.; Graham, G. W.; Pan, X.; Christopher, P. Synthesis of Heteroatom Rh–ReO_x Atomically Dispersed Species on Al₂O₃ and Their Tunable Catalytic Reactivity in Ethylene Hydroformylation. *ACS Catal.* **2019**, *9* (12), 10899–10912.